Preliminary investigations into the theoretical and experimental techniques for exploiting cold atom systems for the purposes of quantum computation

Senior Thesis

Emily Lichko
Advisor: Luming Duan

Contents

Introduction

This thesis seeks to review the basic areas needed to do research on quantum computing in cold atom systems and some preliminary research done by the author in this area. In the first section, the benefits of quantum computation over classical computation were listed and the theoretical underpinnings of quantum computation were briefly reviewed. In the next section, the focus was on cold atom systems, an apparatus that is being developed to implement a quantum computer. The procedures for constructing and manipulating such a system, as well as the procedures for collecting and analyzing information about the system are reviewed in this thesis. The next section involves the current research being done on spinor condensates and quantum spin liquids and in the final section, some preliminary research done by the author in these areas is reviewed.

Theory of Quantum Computation

The main justifications for building a quantum computer are that quantum computers will be able to solve problems more quickly than classical computers and there is the potential for quantum computers to solve problems that classical computers cannot. To quantitatively define

the types of questions that are hard for a classical computer, but easy for a quantum computer, it is necessary to look to a field of computer science called complexity theory. In complexity theory, one is most often interested in functions that have a binary output of the form:

$$f:\{0,1\}^n \rightarrow \{0,1\}$$

For example, if one wanted to know the smallest factor, y, of a given integer x such that $y \neq 1$, we could construct the binary function:

$$f(x,y)=\begin{cases} 1 & \text{if } x \text{ has a divisor } z \text{ such that } z<y \\ 0 & \text{else} \end{cases}$$

and evaluate that function for all integers y, such that $y < x$. The factoring problem is a particularly important problem in a quantum computing, and will come up several times throughout the section [1].

Another important definition in complexity theory is a circuit. A circuit is a set of logical operations (*e.g.* AND, OR, or NOT) that are performed on an input to obtain the output. Circuits are important, because the size of the circuit can be used to quantitatively determine the difficulty of a problem. An important difficulty distinction is given by the following definition, taken from an overview of quantum computation written by John Preskill. "Associated with a family of functions $\{f_n\}$ (where f_n has n-bit input) are circuits $\{C_n\}$ that compute the functions. We say that a circuit family $\{C_n\}$ is "polynomial size" if the size of C_n grows with n no faster than a power of n,

$$\text{size}(C_n) \leq \text{poly}(n),$$

where poly denotes a polynomial. Then we define:

P = {decision problem solved by polynomial-sized circuit families}." [1]

Instead of the distinctions of "easy" and "hard", in complexity theory problems are described by how many steps are necessary to take to solve the problem, given an n-bit input, effectively, how

long it will take to solve the problem. Because problems in P can be solved with poynomial-sized circuit families, in "polynomial time", problems in P are usually considered "easy" to solve [1].

However, most functions of the form $f:\{0,1\}^n \to \{0,1\}$ are not in P. One such type of function is particularly interesting: the set of functions for which, once the answer is found, it is easy it verify, but the answer is not necessarily easy to find. The factoring problem mentioned earlier in the section, for example, is a problem of this type. It takes at most y steps to determine if y is the smallest nontrivial factor of x, however if we are given an integer, z, which someone claims is a smaller nontrivial factor of x, it only takes one step to verify this. This class of problems where the problem may not be easy to solve, but the solution is easy to verify, is called NP, for non-deterministic polynomial time. This type of problem is important to quantum computing, because it is one of the classes of problems where quantum computers can perform better than classical computers. Additionally, the question of whether P = NP is a major unsolved problem in computer science. It is one of the seven Millennium Prize Problems selected by the Clay Mathematics Institute – there is an award of one million dollars for a definitive proof of either P = NP or P ≠ NP. Although there has been no definitive proof as of yet, it is assumed by many mathematicians that P ≠ NP [1, 2].

Now that the basics of complexity theory have been established, we look at two different types of exponential speed-ups that occur when quantum computers are used in the place of classical computers. The first is exponential speed-up relative to a black box and the second is an exponential speed-up for problems that are not in P. A black box, or oracle as it is called in computer science, is a set of unknown unitary operations. By examining a certain number of input and output sets, it is possible to determine which unitary operations are contained in the box.

A good example of a problem which takes exponential time on a classical computer, but can be solved in order-n repetitions for a quantum system is Simon's Problem [1]. In this problem a quantum black box computes the function:

$$f:\{0,1\}^n \rightarrow \{0,1\}^n$$

which as a "period" which is given by an n-bit string, a, such that:

$$f(x)=f(y) \quad iff \quad y=x\circ a$$

In this situation, the operation $\circ$ represents the bit-wise XOR operation, a logical operation that given an input {x, y} flips y if x is 1 and does nothing to y if x is 0.

Classically, to solve this problem, it is necessary to query the oracle an exponentially large amount of times. However, with quantum queries the problem becomes simple. In order to solve this problem quantum mechanically it is necessary to consider the Hadamard transformation:

$$H:|x\rangle \rightarrow \frac{1}{\sqrt{2}}\sum_y (-1)^{xy}|y\rangle$$

First the Hadamard transformation is applied to $|0\rangle$ to get a superposition of all n-bit strings where all n strings are weighted equally:

$$H:|0\rangle \rightarrow \sum_{x=0}^{2^{n-1}} |x\rangle$$

Then this is input into the oracle to obtain:

$$U_f: \sum_{x=0}^{2^{n-1}} |x\rangle|0\rangle \rightarrow \sum_{x=0}^{2^{n-1}} |x\rangle|f(x)\rangle \quad .$$

Then, a measurement is taken on the second register. Let the outcome of the measurement be called $f(x_0)$. Then the state:

$$\frac{1}{\sqrt{2}}(|x\rangle+|x\circ a\rangle)$$

is created in the first register. We can then apply the Hadamard transformation again to obtain the result:

$$H^n:\frac{1}{\sqrt{2}}\left(|x\rangle+|x\circ a\rangle\right)\rightarrow\frac{1}{2^{(n+1)/2}}\sum_{y=0}^{2^n-1}\left[(-1)^{x_0\cdot y}+(-1)^{(x_0\circ a)\cdot y}\right]|y\rangle$$
$$=\frac{1}{2^{(n-1)/2}}\sum_{a\cdot y=0}(-1)^{x_0\cdot y}|y\rangle$$

which is then measured again. The outcome of this measurement must be a value of y such that $a\cdot y=0$. Since the Hadamard gate weights each state equally, there is equal chance of any of the values of y. From here, the problem collapses to a linear algebra problem. If n linearly independent equations of the form $a\cdot y_i=0$ are found then finding a is trivial. The limiting factor in this problem is now the number of measurements that need to be taken on states of the form

$$\frac{1}{2^{(n-1)/2}}\sum_{a\cdot y=0}(-1)^{x_0\cdot y}|y\rangle$$

in order to obtain n linearly independent equations. Since the probability distribution is uniform, on average, this is n iterations. While a classical computer requires exponential time for this problem, a quantum computer can do this in polynomial time [1].

The most famous example of a problem where a quantum computer provides an exponential speed-up for “hard” problems is in the problem of factoring, mentioned earlier in this section. The fastest known classical algorithm used for factoring integers with greater than 100 digits is the general number field sieve. Even using this method, the complexity of the algorithm goes as $O(\exp(c(\ln(n))^{1/3}(\ln(\ln(n)))^{2/3})$, where $O(x)$, means on the order of x [3]. Comparatively, the fastest know quantum algorithm form solving the factoring problem, Shor's algorithm, has a complexity of $O((\ln(n))^3)$, significantly faster than the exponential complexity given for a classical computer[1,4].

Shor's algorithm consists of two parts. First, the factoring problem is mapped to an order-finding problem. Specifically, given that the number to factor is N and its factor is d, a function is defined such that

$$f(x) = a^x \bmod N$$

where a is a randomly selected number such that a < N and gcd(a, N) = 1. If r is defined such that:

$$f(x) = f(x+r) = a^x \bmod N$$

then assuming an r can be found such that r is not odd and $a^{r/2} \neq -1 \bmod N$, then by the Chinese Remainder theorem it is guaranteed that gcd($a^{r/2} \pm 1$, N) = d is a nontrivial factor of N. So for a randomly chosen a < N that fits the conditions mentioned above, if the value of r can be found then d can be found [4].

In order to find r, it is necessary to implement the quantum part of the algorithm. This process is similar to the solution of Simon's problem. First, a superposition of states is created using a Hadamard gate. Then f(x), as defined above is constructed as a quantum function and applied to the superposition of states to obtain a formula of the form:

$$\sum_{x=0}^{Q} |x\rangle|0\rangle \rightarrow \sum_{x=0}^{Q} |x\rangle|f(x)\rangle \quad ,$$

where the superposition of states is the first register and Q is the number of quantum states. Then, a quantum Fourier transform is applied and a measurement of the result is taken. This measurement will r within a certain probability, otherwise another state must be prepared using the Hadamard gate, and the process repeated. However, because of the efficiency of the quantum Fourier transform, this entire process takes on the order of $(\ln(n))^3$ steps [1,4].

This example is famous in part because of the idea that it is very difficult to factor large numbers is the basis for public key encryption. Public key encryption is so named because while

the method for encrypting the data is available to many people, once encrypted, the data cannot be decoded unless the decoder has a “key”, which is available only to a few people. It is used widely in financial transactions, such as for sending credit card information over the internet. One of the most well-known public key encryption schemes is RSA (Rivest, Shamir, Adleman) encryption [1].

RSA encryption is performed by the following algorithm. First, two large prime numbers p and q are selected and N = pq is computed. Then φ(N) = (p -1)(q-1) is computed, where φ(N) gives the number of numbers less than N that are coprime with N. A number e such that e < φ(N) is selected such that e is coprime with φ(N). Suppose Alice wants to sent Bob a message. Bob chooses the values for p and q and Alice receives e and N to encode her message. Given Alice wants to send Bob a message, a, she encodes it using N and e:

$$b = f(a) = a^e (mod\ N)$$

and then sends b to Bob. Once Bob receives b, he can decode it by applying the following operations with the quantity d, which is defined by:

$$ed = 1 (mod\ \phi(N)) \quad ,$$

to get:

$$f^{-1}(b) = b^d (mod\ N) = (a^e)^d (mod\ N) = a^{\phi(N)+1} (mod\ N) = a (mod\ N) \quad .$$

So, Alice can encode her message with e and N, and unless someone is able to find φ(N), or p and q, it is effectively impossible to decode Alice's message [1].

Because the security of public key encryption is used in so many important transactions and can be broken in its current form by Shor's algorithm, a new area of study, quantum cryptography, has been formed. This has led to the development of a technique called quantum key distribution. It is the following advantages over public key encryption systems:

1. Given that party A is trying to communicate with party B, if a third party, E, tries to access the communication, parties A and B will know.
2. Its security rests on the principles of quantum mechanics, not the difficulty of factoring large numbers, so the chances of it being broken are the same as the chances of quantum mechanics being an incorrect theory.

Once this key is established, any type of encryption can be used to encode the message [1].

Cooling, Trapping, Data Collection and Analysis Techniques

There are currently many physical systems that are being explored as possible options for a quantum computer. Due to the fact that nuclear magnetic resonance (NMR) technology was significantly more advanced at the time than the magnetic and optical schemes for quantum computing, some of the earliest implementations of a quantum computer used an NMR system. In an NMR computer, the qubits are the spin states of the molecules and operations are performed by applying radiofrequency (rf) pulses. In 2001, Shor's algorithm was successfully implemented in a seven qubit NMR quantum computer by researchers at IBM [5]. Recently, however, due to experimental advances, the focus in quantum computing has shifted from NMR systems to condensed matter and ultracold gas systems [1, 6, 7].

Condensed matter systems, such at the diamond nitrogen vacancy center system, are also being investigated for use in quantum computing. In this system, the qubits are formed by the point defects were a nitrogen atom replaces a carbon atom and can be manipulated by applying a magnetic field, an electric field, microwave radiation, light, or some combination thereof [6, 7].

There is a broad variety of systems that could be used as a quantum computer, but the system that is the focus of this thesis is the same system that received the 2012 Nobel Prize in Physics, the cold atom system. Atoms are used as the qubits and they are controlled using a magnetic field, light, or some combination thereof. Because of the low temperatures, and thus kinetic energies, that these experiments are performed at, experiments involving cold atoms are considered experimental realizations of many-body Hamiltonians and are thus called quantum simulations [8].

In this next section, I will go over the experimental advances that made quantum computing with cold atoms possible; the different types of of set-ups, or traps, that can be used to contain and manipulate the atoms; and the most commonly used methods for collecting and analyzing information about the atoms in the traps.

Cooling Techniques:

There are several advances that have made cold atom quantum computing possible, but the most important are the advances in cooling techniques. While there is no lower bound in gas density, for quantum computing it is necessary to have a gas density of $n \approx 10^{13}$ cm^{-3}. If the density is greater than 10^{15} cm^{-3}, then the gas will dissipate before it can rethermalize from elastic collisions and if the density is less than 10^{12} cm^{-3}, the thermalization rate of the gas again is too slow when compared to the lifetime of the gas. The density of the gas necessary for the proper rethermalization rates puts a bound on the energy and length scales over which experiments on a gas can be performed. Because the energy is proportional to the temperature, the experiments must be performed in a certain temperature range [8]. Here, we will review some of the most important cooling techniques.

While there are a variety of different techniques that make cold atom quantum computing possible, the techniques of evaporative cooling and laser cooling are responsible, in conjunction with other techniques, for the vast majority of atomic cooling in this kind of experiment. Evaporative cooling involves removing the high-energy atoms from the trap, causing the average energy, and therefore temperature, of a gas to decrease. The limiting factor for evaporative cooling is the ratio of the lifetime of the sample to the collisional thermalization time. The lifetime of the sample must be much longer than the thermalization time in order for evaporative cooling to be effective [6, 7, 8].

A valuable technique of this type is radiofrequency (rf) induced evaporation, because the evaporation process can be separated from the trapping potential. Additionally, rf evaporation is very efficient. The way that rf evaporation works is that the rf pulse flips the spin of the atoms, causing the formerly attractive potential into a repulsive potential. The resonance frequency of the trap is proportional to the magnetic field by the equation:

$$|g|\mu_B B = \hbar\,\omega_{rf}$$

where g is the Landé g-factor, μ_B is the Bohr magneton, B is the magnitude of the magnetic field, $\hbar$ is Plank's constant, and ω_{rf} is the resonance frequency. This equation is for transitions between magnetic sublevels.

The trapping potential U is given by:

$$U = m_F\, g\,\mu_B [B(r) - B(0)]$$

So atoms with energy E > U will evaporate. This gives us:

$$E > U$$
$$E > m_F\, g\,\mu_B [B(r) - B(0)]$$
$$E > \hbar\, m_F (\omega_{rf} - \omega_0)$$

where ω) is the frequency of the rf radiation. This technique, along with laser cooling, is one of the standard methods of atomic cooling [7].

Similarly to evaporative cooling, there are many types of laser cooling. One of the most commonly used techniques for laser cooling is Doppler cooling. A laser is chosen to have an optical frequency which is slightly lower than the atomic resonance. An atom in the trap that is moving away from the beam source will then, due to the Doppler effect, see the laser light at a frequency which is shifter lower than the original frequency. Because it is now lower than the original frequency, that atom will not absorb a photon. Atoms that are moving towards the beam source, on the other hand, will see the light blue-shifted, the frequency of the light will be perceived by the atom to be increased. Because of the increase in perceived frequency, the atom will absorb a photon, slowing the atom. When the photon is emitted from the atom, it is emitted in a random direction, so the overall effect is to reduce the momentum of the gas. Since the momentum of the gas cloud is related to the kinetic energy, and therefore the temperature of the gas, the net effect of the Doppler cooling is to decrease the temperature of the gas along the axis of the beam. To slow atoms of different speeds, the frequency of the laser sweeps through the atomic resonances [6,7, 8, 10].

Two commonly used variants on Doppler laser cooling are Doppler molasses and Zeeman slowing. Doppler molasses is the same process as the standard Doppler laser cooling, but six laser beams oriented in different directions are used instead of one in order to cool the gas more effectively. Zeeman slowing is a variant on Doppler laser cooling where instead of changing the difference between the resonant frequency of the atom and the optical frequency, an inhomogeneous magnetic field is applied. Additionally, optical cooling makes possible the process of sympathetic cooling, where optically cooled atoms are used to cool nearby atoms [6,

7].

The usual experimental technique for loading atoms into a trap involves some sort of pre-cooling, the some combination of a type of evaporative of optical cooling. If the end goal is to hold the gas in an optical trap, the gas will then be loaded into a magnetic trap for further evaporative cooling before it is loaded into the optical trap. Pre-cooling techniques aim to collect a large number of atoms and to obtain high elastic collision rates. These tow objectives are to improve the efficiency of evaporative cooling and because it is easier to transfer larger atomic clouds into magnetic traps without significantly changing the density [6, 7].

Trapping Techniques:

In this next section, we will review that different types of traps that are used to hold the ultracold atoms for manipulation. First, the effects of magnetic trapping on the atomic gas, and then some basic forms of magnetic trapping will be discussed, including the Ioffe-Pritchard configuration. The rest of the section will focus on optical traps. Single beam traps, hybrid traps, and the crossed dipole traps will be briefly covered, but the majority of the section of optical traps will focus on optical lattices. Special attention to optical lattices, because they are important for containing spinor Bose Einstein Condensates (BEC).

Magnetic Trapping:

When a magnetic field is applied in the area around the atomic cloud, an additional term is added to the Hamiltonian,

$$H_B = -\hat{\mu} \cdot B$$

where the μ is the magnetic dipole operator and B is the external magnetic field. This results in the Zeeman energy shifts for the cold atoms:

$$E(m_F) = g\mu_B m_F B$$

where m_F is the magnetic quantum number, μ_B is the Bohr magneton, and g is Lande's factor. For an atom trap $E(m_F)$ must be at a local minimum. For weak field-seeking states, this means that B must be at a minimum for trapping to occur, while for strong field-seeking states trapping by a static magnetic field is not possible. Since only weak field-seeking states can be confined in a magnetic trap, in order for a trap to be stable, the atom's magnetic moment must follow the direction of the magnetic field. This condition can be rewritten as:

$$\frac{d\theta}{dt} < \frac{\mu_m |B|}{\hbar} = \omega_{Larmor}$$

So the Larmor frequency is the upper bound for the rate of change of the field's direction that will sustain a magnetic trap [6, 7, 8].

The Ioffe-Pritchard traps are a combination of a magnetic quadrupole trap with a magnetic bias field along the z – axis, giving to the field configuration:

$$B(x, y, z) = B_0 \begin{bmatrix} 0 \\ 0 \\ 1 \end{bmatrix} + B' \begin{bmatrix} x \\ -y \\ 0 \end{bmatrix} + B'' \begin{bmatrix} -xz \\ -yz \\ z^2 - x^2/2 - y^2/2 \end{bmatrix},$$

where B_0 is the holding field, B' is the quadrupole gradient, and B" is the dipole field curvature. For temperatures $k_B T < \mu_m B_0$, the trap is effectively a harmonic potential, whereas for $k_B T > \mu_m B_0$ the cloud experiences a linear trapping potential in the radial direction. The trapping is still harmonic in the axial direction. For condensates, there are points along the axis of the trip where the B' and the B" term interfere destructively with each other and the trap can no longer confine

the atoms. These points of interference are important considerations when loading the atoms into the trap [6, 7, 8].

Optical Trapping:

There are a variety of benefits to using optical traps in the place of magnetic traps. Unlike magnetic traps, such as the Ioffe-Pritchard configuration, which can confine only weak field-seeking states, optical traps can confine both weak and high field-seeking states. Additionally, trapping atoms optically allows the magnetic field to be used to manipulate the atoms in other ways, such as tuning them to Feschbach resonances.

The simplest optical trap is the single beam laser. The trapping potential for this type of trap is given by the AC Stark shift:

$$U(r)=\frac{-\hbar\omega_R^2(r)}{4}\left(\frac{1}{\omega_0-\omega_L}+\frac{1}{\omega_0+\omega_L}\right)\simeq\frac{\hbar\omega_R^2(r)}{4\Delta}$$

where ω_0 is the atomic frequency, ω_L is the frequency of the laser trap's light, ω_R is the position-dependent Rabi frequency, and $\Delta = \omega_L - \omega_0$ is the laser's detuning. The ω_R term determines the strength of the coupling between the atom and the field. Similarly to most other trapping potentials, the bottom of the single beam trap can be approximated by a harmonic potential. The trapping frequencies in this limit are given as:

$$\frac{\omega_p}{2\pi}=\sqrt{\frac{2P}{\pi^3 m w^4}}$$
$$\frac{\omega_z}{2\pi}=\sqrt{\frac{P}{\pi^3 m w^2 z_R^2}}$$

where P is the laser power, w the beam waist radius and z_R is the Rayleigh range. These are the

parameters used to characterize the beam and which determine the trap depth [6, 7].

A variation on the single beam trap is called a hybrid trap. The main difference between the two traps is an additional magnetic field in the hybrid trap which is applied in order to minimize the aspect ratio, the ratio between the radial and axial trapping frequencies, for optical traps with a large beam waist. An important consideration in choosing the beam waist and the laser intensity are the resultant trap depth. This is especially true when the atomic cloud needs to be cooled by evaporative cooling. In this limit it is necessary for the trap depth to be close to the Fermi energy, which severely limits the size of the beam waist. Another important type of trap to consider is the crossed dipole trap. Besides the historic significance, the first all-optically contained BEC was realized by this type of trap, this type of trap can be useful in transferring a cloud of atoms from a MOT into an optical potential [6, 7].

Some of the most interesting experiments on cold atoms are being done in optical lattices, optical traps that involve multiple interfering laser beams. When the intensity of the beams is sufficiently weak, it is possible for the confined atoms to tunnel between neighboring wells in the lattice configuration. There is a enormous variety of different optical lattice configurations. The most basic configuration for an optical lattices is called a square lattice, and is given by the potential:

$$V_g(x) = V_0^x \cos^2(k_x x) + V_0^y \cos^2(k_y y) + V_0^z \cos^2(k_z z)$$

where the V^i_0 are the magnitudes of the potential in the i direction and the k_i are the wave numbers in the ith direction. It is not just the intensity of the laser beam that defines a certain type of optical lattices, but also the polarization of the beam. By controlling the relative polarizations of the beam it is possible to generate entanglement between the spin states of the atoms and the motion states, leading to phenomena like “spin-dependent transport” [6, 7, 8].

Taking Data:

Unlike for condensed matter quantum computing devices, the vast majority of all data-collecting techniques used with cold gases are optical. Additionally, because the measurements performed on a gas influences the evolution of the gas systems, most measurements can only be performed once on a system. Efficiency is the most vital factor in these types of measurements. However, by using the appropriate imaging methods, it is possible to extract information about the atomic gas by observing the absorption, phase shift, and polarization state of the optical probe. This is the type of information that can be obtained using the imaging techniques described in the next section. More specifically, the section will focus mainly on absorption and dispersive imaging (for both *in-situ* and time-of-flight imaging). It will briefly touch on other considerations in imaging, such as fluorescence imaging, the effects of optical pumping, and imaging in inhomogeneous magnetic fields [6, 7, 8, 9].

Absorption imaging is performed by measuring the fractional transmission of a probe light onto each pixel of a CCD camera, T(ρ), where ρ is the position of the pixel. The image is normalized by comparing the values for T(ρ) with and without the atomic cloud in front of the camera. In the simplest approximation of the experimental setup the areal density of the gas is given by:

$$n_A(\rho) = \frac{-\ln(T(\rho))}{\sigma} \quad ,$$

where σ is the light absorption cross-section. This picture is complicated by factors that will be addressed later in the section, such as optical pumping. A similar technique is called fluorescence imaging, where one differentiates between mission and counted photons. It is free from

background noise, but the strength of the imaging signal can be up to 100 times lower than standard absorption imaging. The primary advantage to absorption imaging is that the measurement has a very high signal – to – noise ratio, as the measurement from any single atom can scatter multiple photons during the optical probing [6, 7, 8].

However, there are drawbacks as well. Since the photon scattering involves a significant change in momentum to the atoms in the gas, once an absorptive image has been taken, the system must be discarded and a new cloud of atoms must be cooled and trapped in the proper potential. Additionally, dense clouds of atoms, the imaging noise increases to the point the uncertainty is too high to measure the cloud density with any reasonable amount of confidence. It is for this reason that absorption imaging is typically used to measure gases after they have been released from a trap, a technique known as *ex-situ* or time of flight imaging. (Taking measurements of atoms in a trap is know as *in-situ* imaging.) [6, 7, 8, 9]

Dispersive imaging, on the other hand, is commonly used to image optically dense atomic clouds in a trap. Dispersive imaging involves observing the phase shift in the laser light due to the light passing through the atomic cloud. Because of this, dispersive imaging requires an ability to separate the scattered and unscattered components of the incoming light. The simplest method of achieving this, called dark-ground imaging, involves blocking the unscattered light from reentering the camera with a filter. This gives the following formulas:

$$E = tE_0 e^{i\phi} = E_0 + \delta E$$
$$\langle I_{dg} \rangle = \frac{1}{2}|E - E_0|^2 = I_0[1 + t^2 - 2\cos(\phi)]$$

The first is for the radiation and the second is for the resultant signal [6, 7, 8].

An extension to this method is called phase-contrast imaging, which is superior to dark-

ground imaging for small φ. It involves shifting the unscattered light by ±π/2 in the Fourier plane of the imaging lens. This light is then interfered with the scattered radiation, which gives an intensity of a point in the image plane as:

$$\langle I_{pc}\rangle = \frac{1}{2}|E - E_0(e^{\pm i\pi/2} - 1)|^2 = I_0[t^2 + 2 - 2\sqrt{2}\cos(\phi \pm \pi/4)]$$

and for small φ:

$$\langle I_{pc}\rangle = I_0[t^2 + 2 - 2t \pm 2t\phi] \quad .$$

In order to determine the efficiency of these techniques, we look at the ratio of signal to heating. In this dimension, dispersive imaging again has an advantage over absorptive heating. The strength of the signal is dispersive imaging is roughly given by:

$$N\frac{\lambda^2}{d^2} \simeq \tilde{n}\lambda^2$$

where $\frac{\lambda^2}{d^2}$ is the solid angle of the diffraction cone and N is the ratio of scattered photons to absorbed photons. Since this is about equal to the optical density, $\tilde{D}_0$, this means that dispersive imaging is approximately 100 times more effective for the same amount of heating[6, 7, 8].

In addition to absorptive and dispersive imaging techniques, there are other considerations. One such consideration is optical pumping. Ideally, the most photons possible would be scattered off the atom to increase the signal to noise ratio. Heating considerations prohibit this from happening. Optical pumping can be used to transition atoms to a state where they can be imaged by the probe. The other consideration comes from imaging in inhomogeneous magnetic fields. Specifically, in the event that the temperature of the cloud exceeds the “natural linewidth”, the inhomogeneous magnetic field can be used to adjust the

resonance of the atoms. This eliminates the need to take into consideration the spectroscopic nature of light scattering [6, 7, 8].

Analysis of Data

Due to the methods described in the section above, it is possible to obtain density distributions of the atomic cloud. From these density distributions, it is possible to infer all the relevant properties of cold atom systems. In order to determine these properties, the observed density distribution is compared to theoretical models of the density distribution of the atomic gas. There are several limits for which the theoretical models of the density distributions are well-documented and experimentally verified. We know that the theoretical models are exactly true for ideal gases ($T \geq T_C$, where T_C is the temperature at which a condensate forms) and for pure condensates. So for high temperatures and very low temperatures, the behavior of the gas is known, but in the intermediate region, it is necessary to use approximations to determine the distributions. The expansion of the strongly interacting atomic gas after it is released from the trap is another area in which physical data about the gas can give information about the interactions within the gas, but a detailed description of this is beyond the scope of this work. In this section, only the ideal gas limit and the condensate limit will be discussed to give an idea of the type of density distributions that are compared with experiment.

The first assumption in the ideal gas limit is that the system is in contact with a reservoir, so that the grand-canonical model can be applied. This is assumed despite the fact that the atom cloud is isolated from its surroundings [8]. The average state of occupation is then obtained to be the standard average occupation for a Bose-Einstein or Fermi-Dirac distribution:

$$\langle n_i \rangle = \frac{1}{e^{\frac{(E_i - \mu)}{K_b T}} \mp 1}, \quad where\, the - is\, for\, bosons\,,\, the + \, for\, fermions$$

Assuming that the particles are in a harmonic trap with the potential:

$$U(r)=\frac{1}{2}m(\omega_x^2 x^2+\omega_y^2 y^2+\omega_z^2 z^2)$$

the Thomas-Fermi approximation is then applied. This approximation assumes that $k_B T = 1/\beta >> \hbar \omega_{x,y,z}$. From this, the occupation of a given unit of phase space, f(r, p) can be obtained. The relationship between the f(r, p) and the density distribution of a thermal gas, $n_{th}(r)$, is given by:

$$n_{th}(r)=\frac{\int d^3 p}{(2\pi h)^3} f(r, p)$$

So for the result obtained for f(r, p), the density distribution of a thermal gas is given by:

$$n_{th}(r)=\pm\frac{1}{\lambda_{dB}^3} Li_{3/2}(\pm e^{\beta(\mu-U(r))})$$

$$where \quad \lambda_{dB}=\sqrt{\frac{2\pi\hbar}{m k_B T}}$$

Quantum effects come into play when the de Broglie wavelength is on the order of the inter-particle spacing, or $\lambda_{dB}=n^{-1/3}$. This is also the point at which a Bose-Einstein condensate (BEC) forms. The density distribution for the ideal gas condensate for bosons is given by:

$$n_c(r)=\frac{N}{\pi^{3/2} dx\, dy\, dz} e^{-\sum_j \frac{x_j^2}{d_j^2}}$$

In the limit that the number of condensed bosons, $N_0 >> 1$, the chemical potential approaches the ground state energy, so with the chemical potential set to zero, the expression for the density of bosons in a trap is obtained to be:

$$n_{th}(r)=\frac{1}{\lambda_{dB}^3} Li_{3/2}(e^{\frac{-U(r)}{k_B T}}) \quad .$$

For fermions on the other hand, the occupation of available phase space scales smoothly to unity. Using the same method as in the Thomas-Fermi limit for an ideal gas, the density profile of

fermions is found to be:

$$n_F(r) = \frac{1}{6\pi}\left(\frac{2m}{\hbar^2}\right)^{3/2}(\mu - U(r))^{3/2} \quad .$$

By comparing these density distributions with the imaging methods from the previous section, information about the static quantities, such as temperature, can be extracted [6, 7, 8].

Spinor BEC and Quantum Spin Liquids:

While magnetic traps have many uses, for quantum computing with atoms, it is necessary to have the spins free in order to be able to manipulate them as qubits. It is for this reason that optical traps are a necessary part of quantum computation. In earlier sections, the methods for optical cold atom confinement have been reviews, but in this next section the methods for probing a spinor BEC and current research into the physics behind spinor BEC's and quantum spin liquids is reviewed.

The spinor condensate is primarily probed using a combination of time-of-flight imaging and Stern – Gerlach spin separation. Once the atomic cloud is cooled down to a condensate and trapped in an optical potential, the optical potential is turned off, and the gas expands for a certain amount of time. Then, a magnetic field gradients is applied, separating the spin state populations. Optical pumping is used to ensure that all of the atoms are in the correct states for the time-of-flight imaging, then they are optically probed. Studies have been done that show that for a F = 1 spinor system, no matter the original distribution of spin states (m_F = 0, 1, -1), after the spinor condensate is allowed to equilibrate, spin relaxation leads to a state where all three spin states are present. The spin states present, however, can be controlled by the application of a magnetic field. For a spinor condensate with m_F = 0, a homogeneous linear magnetic field will have no effect on the spin states, but a field gradient will cause a linear Zeeman shift, which

makes collisions between atoms more favorable and leads to a $m_F = +1$ cloud on the higher-field side of the cloud, and a $m_F = -1$ on the lower field side. Given the polarized condensate described above, now when a homogeneous field is applied, a quadratic Zeeman shift occurs, and in between the $m_F = +1$ and the $m_F = -1$ condensates, a $m_F = 0$ section occurs, because the energy shift causes the energy of a $m_F = 0$ atom to be less than the energies of atoms of other spin states [6, 7].

An important consideration in spinor condensates is whether atoms of different spins will mix, or whether they will be immiscible. This can be determined by looking at the mean field theory for condensates. For a condensate with two different spin states, if the condensates overlap, the energy of the system will be given by:

$$E_O = \frac{2\pi\hbar^2}{m}\frac{N^2}{V}(a_a + a_b + 2a_{ab})$$

If they phase – separate, on the other hand, the energy is:

$$E_S = \frac{2\pi\hbar^2}{m}\left(\frac{N^2}{V_a}a_a + \frac{N^2}{V_b}a_b\right)$$

where in both these equations, a_i is the scattering length of condensate i. Since the condensates will mix if $E_O < E_S$ and will separate otherwise, in terms of the scattering lengths of the condensates, the condition for phase-separation is $a_{ab} > \sqrt{a_a a_b}$ and for mixing it is $a_{ab} < \sqrt{a_a a_b}$ [6, 7].

Now that the methods for experimentally creating a probing a spinor condensate have been reviewed, the next section will focus on recent experimental progress with spinor condensates. Much of the research focuses in an area that relates to frustration of spins in optical lattices. Frustration occurs when opposing forces cannot be satisfied at the same time. The canonical example of spin frustration involves spins placed on the vertices of a triangle. Because

there are three vertices, the spins cannot be anti-aligned with each other, there must be two spins which are either both up or both down that share an edge. For large groups of spins that are frustrated in this way, there is some fluctuation where spins will flip themselves in order to find a lower energy configuration. If the quantum fluctuations are strong enough, the system becomes a quantum spin liquid (QSL), where the spins are highly entangled. This kind of frustration occurs in condensed matter systems, but it also occurs in frustrated lattices for ultracold atoms. This kind of entanglement is necessary for some types of quantum computing, so these types of systems are of particular interest to those interested in quantum computing [11, 12, 13].

There are many different types of QSLs, but one thing that they all are expected to have in common is that they support exotic states, states of matter that cannon be constructed from elementary excitations that are electron-like or magnon-like. The most common exotic excitation found in a QSL is a spinon (S = ½, neutral). While there are a variety of types of QSLs in theory, identifying them experimentally has been difficult. There are many indications of QSLs, a large frustration parameter, the absence of static moments, but there is no "smoking gun" for QSLs as there are for BEC. A complicating factor in the search for QSLs is spin-orbit coupling. It is not known exactly the relation between QSLs and spin-orbit coupling, but in the vast majority of QSL candidates, spin-orbit effects are non-negligible. While it may complicate the search for QSLs, materials with strong spin-orbit coupling and weak correlation have great potential in relation to topological insulators [11, 12].

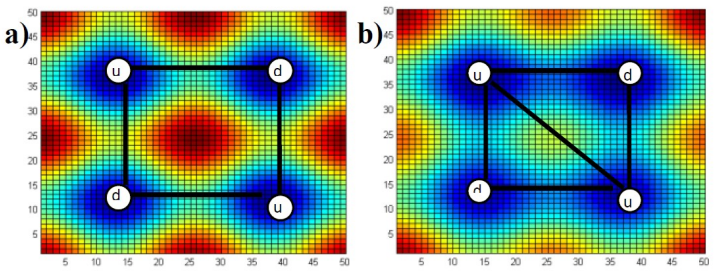

Figure 1: *The diagram to the left shows an example of a non-frustrated spin configuration in a standard square optical lattice. The lines represent the possibility of tunneling and the u and d represent a spin up and a spin down respectively. The diagram to the right shows a frustrated spin configuration in a modified square lattice.*

Preliminary Research:

The culmination of this reading is two small projects done

with the design of optical lattices. The first looked at the hopping rate for atoms contained in wells in optical lattices. The lattices that was used for this project was the square lattice. The standard square lattice is constructed using two laser beams and the resultant potential resembles the image to the left in Figure 1. The heights of the potential maxima are all the same level. This project involved looking into a variation on the standard square lattice that is constructed using three interfering beams. The third beam is used to modulate the height of the center potential. Just as in the image to the right in Figure 1, every other maxima is lower than the global maxima by some factor c, where $c < 1$.

Usually, the potential at the maxima of a square lattice is high enough to prohibit tunneling between wells. However, with the modulated height of the center maxima, it is possible for tunneling to occur across the central, modified, maxima. In the standard square lattice, it was relatively easy for the spins to reach a non-frustrated equilibrium. In the modified square lattice, however, because of the lowered central potential, tunneling is possible along two additional directions in the unit lattice shown in Figure 1. Because of the additional tunneling states, there is no spin equilibrium possible, and the possibility to find a quantum spin liquid emerges.

For this project, I practiced calculating the hopping rate, J, analytically, using a variety of techniques, including the WKB approximation. The most success was had from an implementation of the Wannier functions. One of the graduate students in Luming's lab, Yang Hao Chan, performed the analysis to determine whether there was a spin liquid phase possible in this configuration. He discovered that it was indeed possible for a small set of the parameter space.

The second small project involved the design of a tunable optical lattices. It was based on

two papers: one on a tunable optical Kagomé lattice and one on a tunable honeycomb lattice [14, 15]. Tunable lattices are useful in that they offer additional control over the trapped atoms and the configuration is easier to implement experimentally. My project was to, from reading the papers, implement a tunable setup that could be modified to produce square, triangular, dimer, honeycomb, 1D chains, and the Kagomé lattices using Mathematica. I was able to do this successfully for all these optical lattice types.

Works Cited

[1] Preskill, J. Lecture Notes. Quantum Computation. California Institute of Technology, Pasadena, CA. Last updated 2001.

[2] P versus NP Problem. Wikipedia. Retrieved from http://en.wikipedia.org/wiki/P_versus_NP_problem.

[3] Number Field Sieve. Wolfram Mathworld. Retrieved from http://mathworld.wolfram.com/NumberFieldSieve.html.

[4] Shor's Algorithm. Wikipedia. Retrieved from http://en.wikipedia.org/wiki/Shor's_algorithm.

[5] Vandersypen, L. M. K., M. Steffen, G. Breyta, C. S. Yannoni, M. H. Sherwood, and I. L. Chuang, Nature, **414**, 883.

[6] Ketterle, W., D. S. Durfree, and D. M. Stamper-Kurn, 1999, in *Bose-Einstein Condensation in Atomic Gases*, International School of Physics “Enrico Fermi” Course 140, edit by M. Inguscio, S. Stringari, and C. Wieman (IOS Press, Amsterdam).

[7] Ketterle, W. and M. W. Zwierlein, 2008, in *Ultracold Fermi Gases*, Proceedings of the International School of Physics “Enrico Fermi” Course CLXIV, edit by M. Inguscio, W. Ketterle, and C. Salomon (IOS Press, Amsterdam).

[8] Stamper-Kurn, D. M. and J. H. Thywissen. "Ultracold Bosonic and Fermionic Gases", (Contemporary Concepts of Condensed Matter Science (Elsevier)), edited by A. Fetter, K. Levin, and D. M. Stamper-Kurn.

[9] Bloch, I. , J. Dalibard, and W. Zwerger., 2008, Rev. Mod. Phys., **80**, 885.

[10] Doppler Cooling. RP Photonics Encyclopaedia. Retrieved from http://www.rp-

photonics.com/doppler_cooling.html.

[11] Balents, L., 2010, Nature, **464**, 199.

[12] Lin, Y.-J., K. Jiménez – García, and I. B. Spielman. 2011, Nature, **471**, 83.

[13] Stamper-Kurn, D. M., H.-J. Miesner, A. P. Chikkatur, S. Inouye, J. Stenger, and W. Ketterle. 1999, Phys. Rev. Lett., **83**, 661.

[14] Jo, G.-B., J. Buzman, C. K. Thomas, P. Hosur, A. Vishwanath, and D. M. Stamper-Kurn. 2011. Phys. Rev. Lett., **108**, 045305.

[15] Tarruel, L., D. Breif, T. Uehlinger, G. Jotzu, and T. Esslinger. 2012. Nature, **483**, 302.